Proc. Natl. Acad. Sci. USA
Vol. 95, pp. 10602–10607, September 1998
Cell Biology

WW domain-mediated interactions reveal a spliceosome-associated protein that binds a third class of proline-rich motif: The proline glycine and methionine-rich motif

MARK T. BEDFORD*, ROBIN REED†, AND PHILI LEDER*‡

*Department of Genetics, Harvard Medical School and Howard Hughes Medical Institute, 200 Longwood Avenue, Boston, Massachusetts 02115; and †Department of Cell Biology, Harvard Medical School, 240 Longwood Avenue Boston, MA 02115

Contributed by Philip Leder, June 23, 1998

ABSTRACT **Pre-mRNA splicing requires the bridging of the 5′ and 3′ ends of the intron. In yeast, this bridging involves interactions between the WW domains in the splicing factor PRP40 and a proline-rich domain in the branchpoint binding protein, BBP. Using a proline-rich domain derived from formin (a product of the murine limb deformity locus), we have identified a family of murine formin binding proteins (FBP's), each of which contains one or more of a special class of tyrosine-rich WW domains. Two of these WW domains, in the proteins FBP11 and FBP21, are strikingly similar to those found in the yeast splicing factor PRP40. We show that FBP21 is present in highly purified spliceosomal complex A, is associated with U2 snRNPs, and colocalizes with splicing factors in nuclear speckle domains. Moreover, FBP21 interacts directly with the U1 snRNP protein U1C, the core snRNP proteins SmB and SmB′, and the branchpoint binding protein SF1/mBBP. Thus, FBP21 may play a role in cross-intron bridging of U1 and U2 snRNPs in the mammalian A complex.**

Many cellular processes require physical interactions between proteins. These interactions appear to be mediated by a limited number of modular domains, including Src homology region 2 (SH2) (1), Src homology region 3 (SH3) (2), plekstrin homology (PH) (3), phosphotyrosine-binding (PTB) (4), PDZ (5), and WW domains. This last domain is characterized by two highly conserved tryptophan residues and a proline residue (6, 7, 8). In the majority of cases, the distance from the first conserved tryptophan residue to the following tryptophan is 23 aa and the distance from the same point to the proline residue is 26 aa (W-21aa-W-2aa-P). The NMR structure of the WW domain of the Yes-kinase-associated protein in complex with its cognate peptide and the crystal structure of the WW domain of the Pin1 protein, a regulator of the cell cycle, were solved recently (9, 10). The WW domain represents a small and compact globular structure that interacts with proline-rich ligands (11, 12, 13). At present, two distinct proline-rich binding motifs, PPPPY (14, 15) and PPLP (11, 12, 16), have been identified.

The proline-rich domain of the formins, molecular isoforms involved in murine limb and kidney development (17, 18), was used recently in a protein–protein interaction assay to identify a class of WW domain-containing proteins, the formin binding proteins (FBPs) (12). Unlike most WW domains, FBPs contain a central aromatic block of three tyrosine residues. This tyrosine triplet also is found in the WW domain of PRP40, a yeast protein required for splicing (19). Two proteins isolated by this assay, FBP11 and FBP21, like the splicing factor PRP40, have two WW domains that are separated by a 15-aa spacer (12). Such similarities suggested that these proteins might themselves be involved in pre-mRNA splicing. Furthermore, recent work in both yeast and mammals suggests that a network of interactions between specific splicing factors—PRP40 bound to the 5′ splice site, SF1/BBP bound to the branch site, and U2AF bound to the 3′ splice site—is established in the spliceosomal complex E (20, 21).

It has been determined that the newly discovered FBP11 protein, like the yeast PRP40 protein, binds the splicing factor SF1/mBBP (11). Here, we report that FBP21 also interacts with SF1/mBBP and, moreover, it binds three other splicing factors, SmB, SmB′, and U1C. These interactions are mediated by the WW domains of FBP21, which recognize a proline, glycine, and methionine-rich (PGM) motif. This motif is present in all four of the splicing factors that interact with FBP21. We also show that FBP21 corresponds to a spliceosome-associated protein that is detected in the spliceosomal complex A and that FBP21 is present in spliceosomes assembled on different pre-mRNAs (AdML and tropomyosin). Immunoprecipitation assays indicate that FBP21 is associated with U2 snRNPs. Together, these studies indicate that FBP21 is a general spliceosomal protein.

MATERIALS AND METHODS

Plasmid Constructions. The generation of FBP11 WW, FBP21 WW, Ld10, WBP1, and YAP WW fusion proteins have been described (11, 12, 14). To produce U1A, U1C, SmB, and SmB′ fusion proteins, HeLa cell cDNA was amplified by PCR and was subcloned into the pGEX2TK expression vector (Pharmacia). PCR primers for U1A were 5′-atggatccatggcagttcccgagacccgc-3′ and 5′-aggaattcctacttcttggcaaaggagat-3′. PCR primers for U1C were 5′-atggatccatgcccaagttttattgtgac-3′ and 5′-aagaattctta-tctgtctggtcgagtcat-3′. PCR primers for SmB and SmB′ were 5′-ggggatccccccctggaagagggactcca-3′ and 5′-aggaattcctagggccttggtgggcgcat-3′. Both splice variants were obtained by using these two primers. Primers were flanked by *Bam*HI and *Eco*RI sites, which were used for subsequent cloning of the inserts into pGEX2TK.

SmB13 was constructed by annealing the two oligonucleotides 5′-gatccggcatgccccctccgggaatgcggcctcctcccctgggtgag-3′ and 5′-aattctcacccaggggggaggaggccgcattcccggaggggggcatgccg-3′ and subcloning into pGEX2TK. The WW domains of FBP21L and FBP30 were amplified from mouse cDNA. PCR primers for FBP21L were 5′-ttggatccaaaaagaagaagaagaagaaagaagct-3′ and 5′-aggaattcctactttccactgtccttactagaaagc-3′. PCR primers

Abbreviations: FBP, formin binding protein; GST, glutathione *S*-transferase; PGM, proline glycine and methionine-rich; WBP, WW domain binding protein; snRNAs, small nuclear RNAs; SAP, spliceosome-associated protein.

Data deposition: The sequences reported in this paper have been deposited in GenBank database [accession nos. AF071185 (human FBP21), AF071184 (mouse FBP21), and AF071186 (mouse WBP11)].

‡To whom reprint requests should be addressed. e-mail: leder@rascal.med.harvard.edu.

The publication costs of this article were defrayed in part by page charge payment. This article must therefore be hereby marked "*advertisement*" in accordance with 18 U.S.C. §1734 solely to indicate this fact.

for FBP30 were 5′-catggatccatgcctgcagctcctgtggta-3′ and 5′-aagaattcttaagcaaggtattggggtaactc-3′. After digestion with *Bam*HI and *Eco*RI, the PCR products were cloned into pGEX2TK.

Preparation of Cell Lysates. A murine fibroblast cell line (NIH3T3) and a human kidney epithelial cell line (293) were grown to 80% confluency on 10-cm plates. After a PBS wash, the cells were lysed in 1 ml of RIPA buffer (0.15 mM NaCl/0.05 mM Tris·HCl, pH 7.2/1% Triton X-100/1% sodium deoxycholate/0.1% SDS). This lysate then was sonicated briefly. For SDS/PAGE analysis, 10 μl of this lysate was loaded per lane.

Purification and Labeling of Fusion Proteins. Glutathione *S*-transferase (GST) fusion proteins were purified as described (22).Purified proteins were labeled with [γ-^{32}P]ATP by using heart muscle kinase (22). For most purposes, 10–50 μg of protein were labeled, and the typical specific activity was $\approx 1 \times 10^6$ cpm/μg.

Expression Screening. A mouse limb cDNA expression library was screened. The construction and screening of this oligo dT primed library was described (12).

cDNA Library Screening. The mouse limb cDNA expression library (described above) was screened by using the cDNA insert of FBP21 as a probe. This partial clone of FBP21 was obtained in a previous expression library screen (12). To obtain the human ORF of FBP21, we carried out a BLAST search (http://www.ncbi.NLM.NIH.gov/blast/) of the expressed sequence tag database. A number of expressed sequence tags were identified, purchased (Genome Systems, St. Louis) sequenced and completely.

Blot Overlay Assay. Blot overlay assays were performed as described (12).

Antibodies. A FBP21 WW domain fusion protein (12) was used as an immunogen in rabbits to generate anti-FBP21 antibodies (α21Ab). Polyclonal antibodies were raised by Covance (Princeton, NJ).

The following mouse mAbs were used: Y12 (23), U1–70K (24), Sap62 (25), and B′′ (26). Sap155 antibodies were raised in rabbits (C. Wang and R.R., unpublished data).

Immunoprecipitation. Immunoprecipitations were carried out by using 50 μl of nuclear extract. Antibodies were prebound to either 30 μl protein G Sepharose or 30 μl protein A trysacryl. Mouse monoclonal supernatants (1.5 ml) (U1–70K, Y12) or rabbit immune sera (20 μl) (Sap155, FBP21) were used for the prebinding. Charged beads were incubated with the nuclear extract for 2 hr at 4°C. Beads were washed three times in 250 mM NaCl and 50 mM Tris (pH8). The immunoprecipitates usually were divided in two. One half was run on a SDS/PAGE gel, was blotted to nitrocellulose, and was probed with the indicated antibody. The other half of the immunoprecipitation also was fractionated on a SDS/PAGE gel and was stained with EtBr to detect small nuclear RNAs (snRNAs). Nuclear extract (2 μl) was run in control lanes.

Mammalian A/B and H Complexes. Mammalian A/B and H complexes were purified as described (27). The complexes were purified by assembling them on biotinylated AdML pre-mRNA, were isolated by gel filtration, and then were affinity-selected by binding to avidin agarose.

Indirect Immunofluorescence. HeLa cells were washed with PBS and were incubated with 3% paraformaldehyde, 0.3% Triton (in PBS) for 5 min at room temperature, then were incubated for 30 min with 3% paraformaldehyde. Cells were washed three times in PBS. The cells then were incubated for 25 min at room temperature with the rabbit αFBP21 antibody diluted 1:1000 in SC35 mouse monoclonal supernatant. Cells then were washed three times with PBS and were incubated for a further 25 min with 1:200 fluorescein-conjugated goat anti-mouse IgG (Jackson ImmunoResearch 715-096-150) and 1:500 Texas Red-conjugated goat anti-rabbit IgG (Jackson ImmunoResearch 711-076-152) diluted in PBS. The secondary antibodies were aspirated, and the cells were rinsed twice with PBS. Samples were observed on a fluorescence microscope (Zeiss). The cross reactivity of the two secondary antibodies was tested for, and they were found not to react with other antigens.

RESULTS

The WW Domain of FBP21 Binds Splicing Factors. FBP21 is one of several proteins identified by their ability to bind the proline-rich domain of formin (12). In turn, a functional interaction screen of a cDNA expression library was used to identify putative ligand partners for the WW domain of FBP21. Eight positive plaques were purified, representing four different proteins. The snRNP core protein SmB (28, 29) accounted for half of the interacting plaques. Another splicing factor, the SF1-HL1 splice variant of SF1/mBBP (30), also was identified. Two plaques encoded an orphan protein, the sequence of which showed no significant similarity to any proteins currently in databases. We have called this protein WW domain binding protein 11 (WBP11). The fourth sequence corresponded to a reported ORF of no known function (accession no. AB000459). In summary, two splicing factors accounted for five of the eight positive plaques identified in the screen.

Apart from the WW domain, FBP21 also contains a zinc finger (Fig. 1*A*). This zinc finger motif displays striking homology to the zinc finger in the U1 snRNP-specific protein U1C (Fig. 1*B*) (31). The observation that FBP21 binds two splicing factors (SmB and SF1/mBBP) and contains two distinct domains found in known splicing factors suggests that FBP21 itself may be involved in splicing.

Further evidence that FBP21 interacts with splicing proteins was obtained in gel overlay assays. Total mouse NIH 3T3 cells or human 293 cell lysates were fractionated by SDS/PAGE, were immobilized on a filter, and were probed with radiolabeled FBP21 WW domain. A strong signal at the expected position of SmB and its splice variant, SmB′, was detected (Fig. 2*A*). To confirm their identity, these two bands also were detected on a duplicate blot probed with the Y12 Ab, an antibody that recognizes both SmB and SmB′ (Fig. 2*A*). Furthermore, SmB and SmB′ were detected in a gel overlay assay of a U1 snRNP immunoprecipitate (Fig. 2*B*). Two additional bands are detected in the U1 snRNP immunoprecipitate. The lower molecular weight band corresponds in size to the U1-specific protein, U1C, which interacts with FBP21

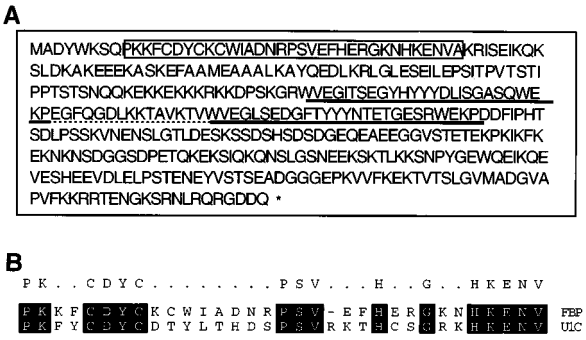

FIG. 1. Predicted amino acid sequence of the FBP21 cDNA reveals a zinc finger motif and two WW domains. (*A*) Amino acid sequence of FBP21. The zinc finger motif is boxed. The two WW domains are underlined with a solid line. The 15-aa spacing between the two WW domains is underlined with a broken line. This spacer distance is conserved between the WW domains of the putative splicing factor FBP11, FBP21, and the yeast U1-associated splicing factor PRP40. (*B*) A BLAST search aligning the zinc finger of the splicing factor U1C with the zinc finger of FBP21. The alignment was the best fit obtained by using the BLAST search.

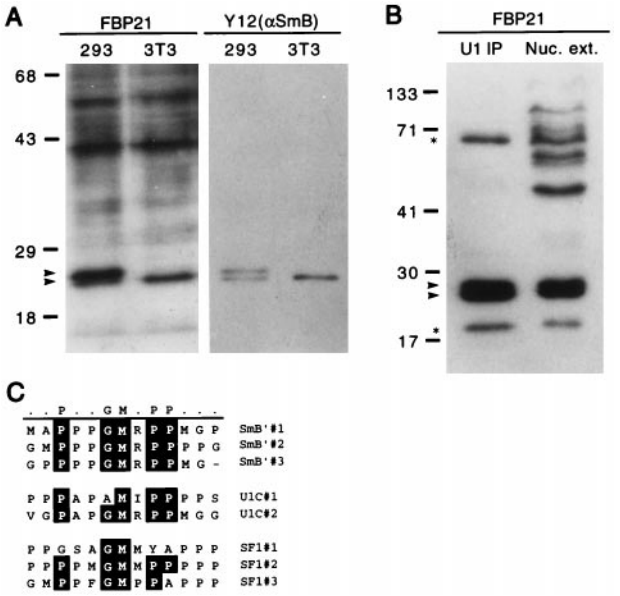

FIG. 2. The WW domain of FBP21 binds SmB as determined by blot overlay. (*A*) Total cell lysate probed with the ^{32}P-GST-FBP21 WW domain. Total cell lysates from 293 cells (a human cell line) and NIH 3T3 cells (a mouse cell line) were prepared in RIPA buffer. Lysates were run on an SDS/PAGE gel, were blotted onto nitrocellulose, and were incubated with radiolabeled GST-FBP21 WW (see *Materials and Methods*). A duplicate blot was incubated with the Y12 antibody to visualize the spliceosomal proteins, SmB, and its variant SmB′. The blot was developed by using enhanced chemiluminescence (ECL, Amersham). The upper arrow identifies SmB′; the lower arrow identifies SmB. (*B*) SmB and SmB′ are detected in HeLa cell nuclear extract (Nuc. ext.) and immunoprecipitates of HeLa cell nuclear extract. Immunoprecipitates were performed with an anti-U170 antibody to "pull down" U1-associated proteins (U1 immunoprecipitates), which were resolved side-by-side on a SDS/PAGE gel, were blotted onto nitrocellulose, and were incubated with radiolabeled GST-FBP21 WW. The upper starred band runs in the expected position of SF1, and the lower starred band runs in the position of U1C. Molecular mass markers (in kDa) are indicated. (*C*) An alignment of SmB′, U1C, and SF1 reveals a motif rich in proline, glycine, and methionine residues. This motif is repeated three times in SmB′ and SF1 (SF1-HL1) and twice in U1C. The alignment was carried out by using the program MEGALIGN (DNAstar, Madison, WI).

(see below) and is a known U1 snRNP protein (Fig. 2*B*, lower starred band). The identity of the higher molecular weight band is not known.

FBP21 WW Domain Ligands Share a Common PGM Motif. Sequence comparisons of the splicing factors SmB′ and SF1/mBBP revealed a common motif that might be responsible for the interactions with FBP21 (Fig. 2*C*). U1C also contains a similar motif (Fig. 2*C*). The latter observation, in conjunction with our data showing that a protein of the size of U1C is detected by FBP21 in the gel overlay assay (Fig. 2*B*) suggested that FBP21 also may interact with U1C. The PGM motif has been described in SmB (and SmB′), U1C, and U1A proteins (28, 29) and is also present in the SF1/mBBP splice variant, which was isolated in our expression library screen and was described by Arning *et al.* (30). The PGM domain is most striking in SmB′, where it is repeated three times (28) (Fig. 2*C* and Fig. 3*A*).

To determine whether this motif binds the WW domains of FBP21, we made three GST-fusion proteins containing elements of this region. These were SmB13, which consists of a 13-aa sequence containing one PGM unit; SmB, which consists of 27 amino acids containing one PGM unit; and SmB′, which consists of 36 amino acids and contains two PGM units (Fig. 3*A*). We also made GST fusion proteins of full-length U1A and U1C. Blot overlay analyses revealed that SmB, SmB′, and U1C

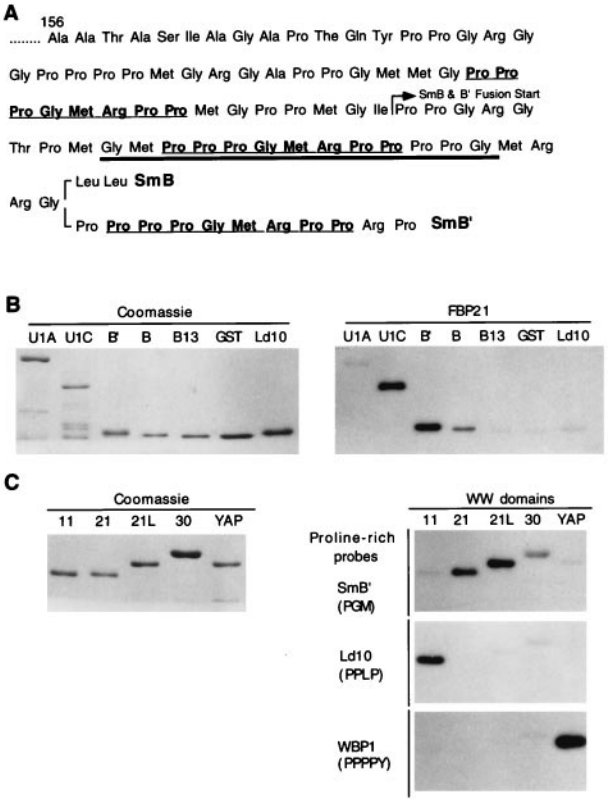

FIG. 3. FBP21 binds with specificity to the splicing factors SmB, SmB′, and U1C. (*A*) Diagram of SmB GST fusion proteins. The PGM motif that is repeated three times is underlined. The start of GST-SmB (26 aa) and GST-SmB′ (35 aa) fusion proteins is indicated with an arrow. The fusion protein that includes one repeat unit (GST-SmB13) is underlined in bold. (*B*) Role of the PGM motif in FBP21 interactions. The indicated purified GST fusion proteins were run on SDS/PAGE gels, and one gel was stained with Coomassie blue whereas the other was blotted to nitrocellulose. The symbols GST, U1A, U1C, B′ (SmB′), and B (SmB) refer to the proteins and peptides described in *Materials and Methods* and above (*A*). The term GST represents the fusion peptide alone. ld10 is a GST fusion containing a 10-aa proline-rich peptide from formin (11). The filter was probed with radiolabeled GST-FBP21 WW. (*C*) The specificity of different WW domains for specific proline-rich sequences. The indicated WW domain-containing GST fusion proteins were purified and were run on SDS/PAGE gels. The lanes were loaded with WW domains from FBP11 (11), FBP21 (21), a longer version of FBP21 containing the same WW domains (21L), the distantly related FBP30 (30) protein (12), and the YES-associated protein (YAP) as described in *Materials and Methods*. One gel was Coomassie blue-stained, and the other three were blotted to nitrocellulose. The filters were probed with radiolabeled GST-SmB′, GST-Ld10, and GST-WBP1 (14), which are representative of PGM, PPLP, and PPPPY proline-rich motifs, respectively.

interact strongly with the FBP21 WW domains (Fig. 3*B*). U1A and GST itself do not bind the labeled fusion protein. Moreover, the FBP11 WW domain ligand ld10, which contains a PPLP motif, does not interact with FBP21, suggesting specificity of ligand recognition. This specificity of interaction exists even though the WW domains of FBP21 and FBP11 are similar in sequence and identical with regard to the distance between the two WW domains (12).

The PGM Motif Interacts Specifically with the WW Domain of FBP21. To assay for specific ligand usage, we tested the binding of a PGM-motif-containing ^{32}P-labeled GST-SmB′ fusion probe to a panel of four different WW domains (Fig. 3*C*). Each lane contained approximately the same amount of GST fusion protein (Fig. 3*C*). SmB′ bound well to two different fusion proteins containing the WW domains of FBP21 (21 and 21L). However, it bound less strongly to the

WW domain of FBP30 (a distantly related WW domain) and did not bind the WW domains of FBP11 or YAP65 (YES-associated protein). Conversely, the ligands for the WW domains of FBP11 and YAP, ld10, and WBP1, respectively (12, 13), only bound their appropriate WW domain targets (Fig. 3C). These results indicate that the PGM motif is a third proline-rich motif that, in addition to PPPPY and PPLP, can be bound by a specific class of WW domain.

FBP21 Coimmunoprecipitates with U2 snRNP. Because FBP21 binds the splicing factors SmB, SmB′, SF1, and U1C, it was not unreasonable to suspect that FBP21 may be associated with one or more of the spliceosomal snRNPs. To address this possibility, we raised polyclonal antibodies to FBP21. To show that the antibodies detected FBP21, two independent human cDNA clones (21a and 21b) that contained the ORF corresponding to FBP21 were *in vitro* translated. Western blot analysis of these translation products, of A/B complex (see below), and of HeLa cell nuclear extracts showed that this antibody (α21Ab) recognizes a single protein of 58 kDa (Fig. 4*A*). No binding of α21Ab to proteins in a control *in vitro* translation reaction was detected (Fig. 4*A*, Lucif. cont.).

To determine whether FBP21 is present in snRNPs, we carried out immunoprecipitations with a series of antibodies against snRNP proteins. The immunoprecipitates were analyzed for proteins and snRNAs. Using α21Ab, Western blot analysis of the immunoprecipitates revealed that FBP21 is present in the Y12 immunoprecipitate. Y12 is directed against SmB and SmB′ and thus immunoprecipitates all splicing snRNAs (U1, U2, U4, U5, and U6) (Fig. 4*B*). FBP21 is not detected in an immunoprecipitate of U1 snRNP alone (Fig. 4*B*; U1–70) under these high salt conditions, but it is detected in immunoprecipitates using antibodies directed against several U2 snRNP proteins [B′′, spliceosome-associated protein (SAP) 62, SAP 155]. We conclude that FBP21 is associated with U2 snRNP.

We note that more FBP21 is detected in the SAP 62 and SAP 155 immunoprecipitates than in the B′′ immunoprecipitate (Fig. 4*B*). A reasonable interpretation of these data is that FBP21 is associated with a specific subpopulation of U2 snRNP. For example, it is known that U2 snRNP exists in a 17S and a 12S form (32). The 17S form contains SF3a/b proteins (i.e., SAPs 62 and 155) (32, 33, 34). Thus, our data are consistent with the possibility that FBP21 is associated with 17S U2 snRNP.

We attempted to demonstrate directly that FBP21 is essential for splicing. However, we were unable to deplete a nuclear extract of endogenous FBP21 or inhibit an *in vitro* splicing reaction with α21Ab. The α21Ab was also unable to immunoprecipitate any of the snRNAs. A likely explanation for these data is that the antibody was raised against the WW domain of FBP21, and the epitope may be masked by protein–protein interactions.

Localization of FBP21 to Nuclear Speckles. All splicing factors characterized to date have been shown to colocalize in nuclear speckle domains *in vivo* (39). Significantly, immunofluorescence studies with αFBP21 Ab demonstrated that endogenous FBP21 is exclusively localized to the nucleus and concentrated in a punctate pattern (Fig. 4*C*). Moreover, FBP21 colocalizes with the essential splicing factor SC35, which is known to localize in nuclear speckle domains (40). Thus, together with the data presented above, this result indicates that FBP21 is a component of the splicing machinery.

FBP21 Is a Spliceosome-Associated Protein. Pre-mRNA splicing takes place in the spliceosome, a highly dynamic complex containing five snRNAs and >50 proteins (for reviews, see refs. 35 and 36). The snRNPs bind to pre-mRNA in a stepwise manner, first forming the E complex (early complex) followed by the A, B, and C complexes. To determine whether FBP21 is a spliceosomal protein, we used α21Ab, the

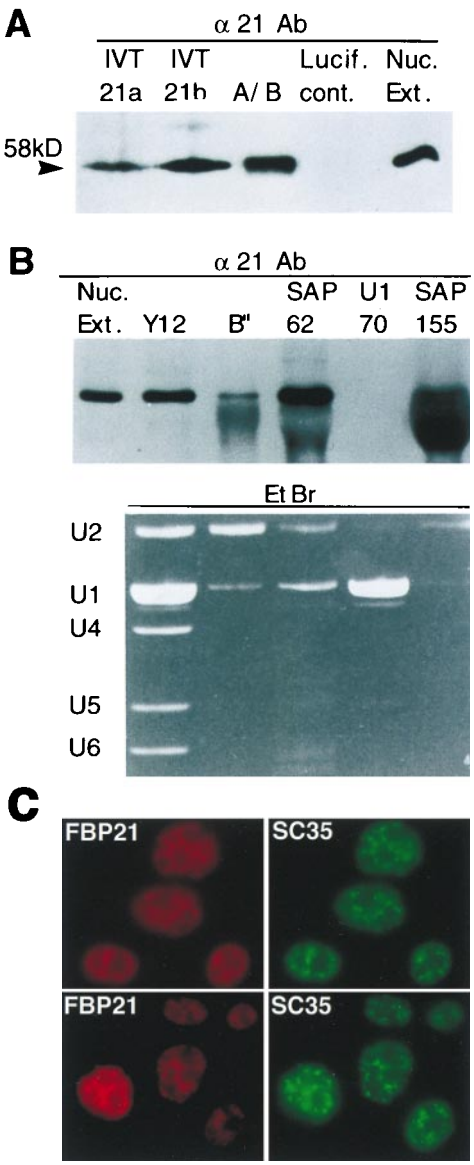

FIG. 4. FBP21 is a 58-kDa protein that is associated with the U2 snRNP. (*A*) Analysis of *in vitro*-translated FBP21. Two different cDNAs (21a and 21b) for FBP21 were transcribed and translated *in vitro* in reticulocyte lysates as described (Promega). Translated products were run on a SDS/PAGE gel with an A/B complex of spliceosome-specific proteins (A/B), a luciferase *in vitro* translation product as a control (Lucif. cont.), and HeLa cell nuclear extract (Nuc. Ext.) and were blotted to nitrocellulose. The filter was probed with the α21Ab antibody. The arrowhead shows the detected band of 58 kDa. (*B*) Association between FBP21 and U2 snRNP's. The indicated antibodies (Y12, anti-SmB, and SmB′; B″, anti-B″; SAP 62, anti-SAP 62; U1–70, anti-U1–70, and SAP 155, anti-SAP 155) were used to perform immunoprecipitations of HeLa cell nuclear extracts under RNase free conditions. The immunoprecipitations were washed three times in a buffer containing 250 mM NaCl and 50 mM Tris (pH8). The immunoprecipitations then were divided in two. One half was run on a SDS/PAGE gel, was blotted to nitrocellulose, and was probed with α21Ab (*Upper*). The other half of the immunoprecipitation also was fractionated on a SDS/PAGE gel and was stained with EtBr to detect snRNAs (*Lower*). The large protein band seen in the SAP 155 lane is Ig heavy chain. A light band corresponding to FBP21 can be seen above it. (*C*) Localization of endogenous FBP21. HeLa cells were fixed, and the cellular localization of FBP21 was determined by indirect immunofluorescence microscopy with αFBP21 antibodies. The FBP21 protein is localized in a speckled nuclear pattern, characteristic of splicing factors. FBP21 colocalizes with SC35, an SR protein that is required for pre-mRNA splicing and is a characterized marker for nuclear speckles. Two different fields are shown. The Texas Red signal represents the endogenous FBP21 protein, and the FITC signal represents SC35 SR protein.

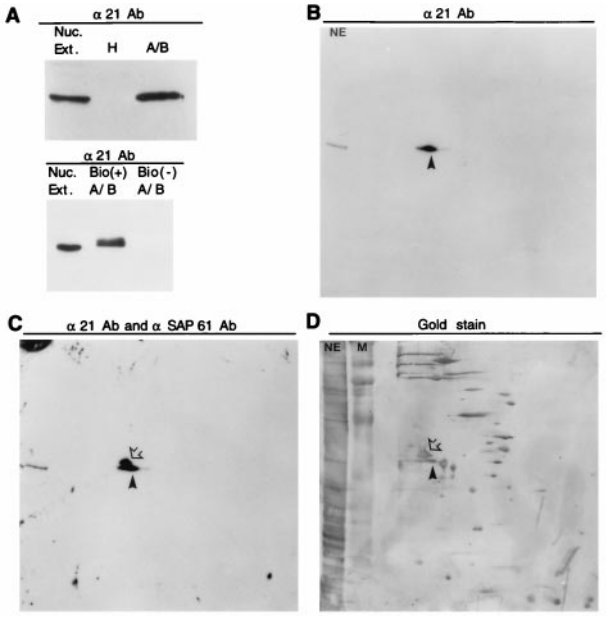

FIG. 5. FBP21 is found in an A/B complex of spliceosome-specific proteins. (*A*) FBP21 is associated with the A/B complex. RNA binding proteins were assembled on AdML pre-mRNA. RNA-protein complexes were size-selected and purified. Two complexes were isolated: the A/B complex [containing spliceosome-specific proteins (snRNPs)] and the H complex (hnRNPs). Nuclear extract and the two complexes were run on an SDS/PAGE gel, were blotted onto nitrocellulose, and were incubated with α21Ab (*Upper*). The A/B complex isolation was repeated by using biotinylated [Bio (+) A/B] RNA and nonbiotinylated RNA [Bio (−) A/B]. Samples were run on a SDS/PAGE gel, were blotted onto nitrocellulose, and were incubated with α21Ab (*Lower*). In both upper and lower, the protein band migrates as 58 kDa. (*B–D*) 2D gel analyses of spliceosome-specific proteins. Spliceosome-specific proteins were fractionated by 2D gel electrophoresis and were blotted to nitrocellulose. (*B*) The filter first was probed with α21Ab. (*C*) It then was reprobed with an antibody against SAP 61, without removing the α21Ab. All blots were developed by using enhanced chemiluminescence (ECL, Amersham). (*D*) The same filter then was gold stained. FBP21 is indicated by the closed arrowhead, and SAP 61 is indicated by the open arrowhead. Marker (M) and HeLa cell nuclear extract (NE) were run in the second dimension.

anti-FBP21 antibody, for Western blot analysis of the A/B complex. The A/B complex was purified by assembling it on biotinylated AdML pre-mRNA and then isolating it by gel filtration followed by affinity selection on avidin agarose (37). FBP21 was detected in the A/B complex, but neither in the hnRNP complex H (Fig. 5*A Upper*) nor in the E complex (data not shown). FBP21 also was detected in the A/B complex assembled on tropomyosin pre-mRNA (data not shown), indicating that FBP21 is a general spliceosomal protein. To determine whether FBP21 was associated specifically with the A/B complex and not with the avidin beads used in the isolation of the complex, we repeated the experiment, assembling the A/B complex on biotinylated or nonbiotinylated RNA. FBP21 was detected only when the RNA was biotinylated, confirming the specificity of this interaction (Fig. 5*A Lower*).

The components of the A/B spliceosomal complex have been identified on 2D gels (38). Western blot analysis of spliceosomes fractionated on a 2D gel shows that FBP21 migrates directly below the spliceosome-associated protein SAP 61 (Fig. 5 *B* and *C*). The spot detected by α21Ab can be superimposed on the gold stain of a hitherto uncharacterized spliceosome-associated protein (Fig. 5*D*), which we now know to be FBP21.

DISCUSSION

The WW Domain of FBP21 Recognizes a PGM Motif. It seems clear that the reciprocally interacting WW and proline-rich domains consist of subtly altered motifs used in a variety of combinations to confer specificity on protein–protein interactions. Seven of the eight interacting sequences we identified contained at least two proline-rich domains that were also abundant in methionine and glycine residues. Given this amino acid content and the above-noted interaction specificity, these domains appear to constitute a subclass characterized by what we term the PGM motif. This motif differs from the proline-rich binding domains found in other WW domain ligands, both in amino acid content and binding specificity (11, 12, 13). Further, only one copy of this motif, with some flanking sequence, is both necessary and sufficient for binding the FBP21 WW domain (Fig. 3*B*, lane B).

The identification of these PGM motifs allows us to speculate regarding the biologic significance of alternatively spliced forms of the splicing factors SmB and SF1. In both of these proteins, alternative splicing alters their proline-rich exon content in a tissue-specific fashion (28, 29, 30, 41). The snRNP proteins SmB and SmB′ differ only at their COOH-terminus, where an additional proline-rich motif is attached in the case of SmB′ through an alternative splicing event (28, 29). The addition of another proline-rich domain enhances the binding of FBP21 to SmB′ (Fig. 3*B*), thereby providing a way of regulating binding affinities. Obviously, such processing may play a role in ligand selection and binding strength.

It has been shown that FBP11 binds a splice variant of SF1/mBBP (ZFM1-B) (11). We demonstrate here that FBP21 recognizes another SF1/mBBP splice variant, SF1-HL1. Seven alternatively spliced forms of SF1 have been described (30). Six of these splice forms encode proteins with a common N-terminal half containing two RNA binding motifs. They all differ, however, in the length and sequence of their proline-rich C-termini. It is possible that the choice of C-termini may regulate both FBP11 and FBP21 interactions with SF1/mBBP.

The FBPs Form a Class of WW Domains Functionally Linked to Splicing. Although the PGM motif represents a specific class of proline-rich WW ligands, the FBPs also form a class of WW domains that possess a distinguishing central aromatic block of three tyrosine residues. These FBP-like WW domains are unlikely to bind the PPPPY motif that is recognized by YAP and NEDD4 WW domains (ref. 13; M.T.B. and P.L., unpublished data) because they were isolated based on their ability to bind a formin proline-rich region that lacked this tyrosine-containing motif (12). Three of the WW domain-containing proteins that can be grouped into the tyrosine-rich FBP WW domain class (W-YYY-W) are linked to splicing. All of these proteins (FBP11, FBP21, and PRP40) bind splicing factors by means of a WW domain-mediated interaction (11, 20). In addition, PRP40 is a U1 snRNP protein that is essential for splicing in yeast (19). In this study, we identify FBP21 as a member of the A/B complex.

A Possible Role for FBP21 in Splicing. Recent work indicates that cross-intron bridging involves protein–protein interactions between the WW domain-containing protein PRP40, which is bound at the 5′ splice site, BBP, which is bound at the branch site, and mud2p, which is bound at the 3′ splice site (20, 21). These interactions are thought to be conserved in mammals, with the corresponding proteins being FBP11, SF1/mBBP, and U2AF^{65}, respectively (11, 20, 21). However, our data show that FBP21, like FBP11, also interacts with SF1/mBBP. Moreover, FBP21 interacts with the snRNP core proteins SmB and SmB′ as well as with the U1 snRNP protein U1C. Finally, FBP21 is associated with U2 snRNPs and is a component of the A/B complex. These data implicate FBP21 in cross-intron bridging.

Because there are now at least two metazoan proteins (FBP11 and FBP21) related to yeast PRP40 and no other PRP40-like protein in yeast, the process for intron bridging in metazoans may be more complicated than in yeast. At least two possible scenarios can be envisioned: Firstly, FBP11, which more closely resembles PRP40 (M.T.B. and P.L., unpublished data), functions in cross-intron bridging in the E complex and then is replaced by FBP21 in the A/B complex. Alternatively, FBP21 and FBP11 may be functionally similar family members that interact with (or are recruited by) different isoforms of SF1 or different pre-mRNA substrates. Further characterization of FBP21, FBP11, and other FBPs will be necessary to distinguish between these possibilities.

U1C is a U1 snRNP-specific protein that can homodimerize (42), thereby providing two potential points of interaction for FBP21. Further, the N-terminal domain of U1C is necessary and sufficient for the early stage of spliceosome assembly (43), possibly leaving the PGM-rich C-terminal domain free for FBP21 binding. SmB and SmB′ also could provide or reinforce this point of contact for cross-intron interactions. It is also possible that FBP21 may not interact directly with either the homodimer of U1C or the two SmB splice variants but rather with a complex of these four proteins that might create a proline-rich field (a "PGM front"), which would interact with high avidity with the two WW domains of FBP21. This high avidity interaction surface would be created only after U1 snRNP binding, thereby providing an element of regulation to this intron-bridging protein cascade.

We thank D. C. Chan for the initial work that formed a basis for this study. We are grateful to C. H. Westphal and B. Weiss for advice in the preparation of this manuscript. M.T.B. is supported in part by Award 1440 of the Cancer Research Fund of the Damon Runyon–Walter Winchell Foundation.

1. Marengere, L. E. & Pawson, T. (1994) *J. Cell. Sci. (Suppl.)* **18,** 97–104.
2. Musacchio, A., Wilmanns, M. & Saraste, M. (1994) *Prog. Biophys. Mol. Biol.* **61,** 283–297.
3. Ferguson, K. M., Lemmon, M. A., Sigler, P. B. & Schlessinger, J. *Nat. Struct. Biol.* **2,** 715–718.
4. Bork, P. & Margolis, B. (1995) *Cell* **80,** 693–694.
5. Songyang, Z., Fanning, A. S., Fu, C., Xu, J., Marfatia, S. M., Chishti, A. H., Crompton, A., Chan, A. C., Anderson, J. M. & Cantley, L. C. (1997) *Science* **275,** 73–77.
6. Andre, B. & Springael, J. Y. (1994) *Biochem. Biophys. Res. Commun.* **205,** 1201–1205.
7. Bork, P. & Sudol, M. (1994) *Trends Biochem. Sci.* **19,** 531–533.
8. Hofmann, K. & Bucher, P. (1995) *FEBS Lett.* **358,** 153–157.
9. Macias, M. J., Hyvonen, M., Baraldi, E., Schultz, J., Sudol, M., Saraste, M. & Oschkinat, H. (1996) *Nature (London)* **382,** 646–649.
10. Ranganathan, R., Lu, K. P., Hunter, T. & Noel, J. P. (1997) *Cell* **89,** 875–886.
11. Bedford, M. T., Chan, D. C. & Leder, P. (1997) *EMBO J.* **16,** 2376–2383.
12. Chan, D. C., Bedford, M. T. & Leder, P. (1996) *EMBO* **15,** 1045–1054.
13. Einbond, A. & Sudol, M. (1996) *FEBS Lett.* **384,** 1–8.
14. Chen, H. I. & Sudol, M. (1995) *Proc. Natl. Acad. Sci. USA* **92,** 7819–7823.
15. Linn, H., Ermekova, K. S., Rentschler, S., Sparks, A. B., Kay, B. K. & Sudol, M. (1997) *Biol. Chem.* **378,** 531–537.
16. Ermekova, K. S., Zambrano, N., Linn, H., Minopoli, G., Gertler, F., Russo. T. & Sudol, M. (1997) *J. Biol. Chem.* **272,** 32869–32877.
17. Woychik, R. P., Maas, R. L., Zeller, R., Vogt, T. F. & Leder, P. (1990) *Nature (London)* **346,** 850–853.
18. Woychik, R. P., Stewart, T. A., Davis, L. G., D'Eustachio, P. & Leder, P. (1985) *Nature (London)* **318,** 36–40.
19. Kao, H. & Siliciano, P. G. (1996) *Mol. Cell. Biol.* **16,** 960–967.
20. Abovich, N. & Rosbash, M. (1997) *Cell* **89,** 403–412.
21. Berglund, J. A., Chua, K., Abovich, N., Reed, R. & Rosbash, M. (1997) *Cell* **89,** 781–787.
22. Kaelin, W. G., Jr., Krek, W., Sellers, W. R., DeCaprio, J. A., Ajchenbaum, F., Fuchs, C. S., Chittenden, T., Li, Y., Farnham, P. J. & Blanar, M. A (1992) *Cell* **70,** 351–364.
23. Billings, P. B., Barton, J. R. & Hoch, S. O. J. (1985) *J. Immunol.* **135,** 428–432.
24. Billings, P. B., Allen, R. W., Jensen, F. C. & Hoch, S. O. (1982) *J. Immunol.* **128,** 1176–1180.
25. Hong, W., Bennett, M., Xiao, Y., Feld Kramer, R., Wang, C. & Reed R (1997) *Nucleic Acids Res.* **25,** 354–361.
26. Habets, W. J., Hoet, M. H., De Jong, B. A., Van der Kemp, A. & Van Venrooij, W. J. (1989) *J. Immunol.* **143,** 2560–2566.
27. Bennett, M. & Reed, R. (1993) *Science* **262,** 105–108.
28. Rokeach, L. A., Jannatipour, M., Haselby, J. A. & Hoch, O. S. (1989) *J. Biol. Chem.* **264,** 5024–5030.
29. van Dam, A., Winkel, I., Zijlstra-Baalbergen, J., Smeenk, R. & Cuypers, H. T. (1989) *EMBO J.* **8,** 3853–3860.
30. Arning, S., Gruter, P., Bilbe, G. & Kramer, A. (1996) *RNA* **2,** 794–810.
31. Nelissen, R. L., Heinrichs, V., Habets, W. J., Simons, F., Luhrmann, R. & van Venrooij, W. J. (1991) *Nucleic Acids Res.* **19,** 449–454.
32. Behrens, S. E., Tyc, K., Kastner, B., Reichelt, J. & Luhrmann, R. (1993) *Mol. Cell. Biol.* **13,** 307–319.
33. Brosi, R., Groning, K., Behrens, S. E., Luhrmann, R. & Kramer, A. (1993) *Science* **262,** 102–105.
34. Staknis, D. & Reed, R. (1994) *Mol. Cell. Biol.* **14,** 2994–3005.
35. Will, C. L. & Luhrmann, R. (1997) *Curr. Opin. Cell Biol.* **9,** 320–328.
36. Kramer, A. (1996) *Annu. Rev. Biochem.* **65,** 367–409.
37. Reed, R. (1990) *Proc. Natl. Acad. Sci. USA* **87,** 8031–8035.
38. Bennett, M., Michaud, S., Kingston, J. & Reed, R. (1992) *Genes Dev.* **6,** 1986–2000.
39. Spector, D. L. (1993) *Curr. Opin. Cell. Biol.* **5,** 442–447.
40. Fu, X. D. & Maniatis, T. (1990) *Nature (London)* **343,** 437–441.
41. Sharpe, N. G., Williams, D. G., Norton, P. & Latchman, D. S. (1989) *FEBS Lett.* **243,** 132–136.
42. Gunnewiek, J. M., van Aarssen, Y., Wassenaar, R., Legrain, P., van Venrooij, W. J. & Nelissen, R. L. (1995) *Nucleic Acids Res.* **23,** 4864–4871.
43. Will, C. L., Rumpler, S., Klein Gunnewiek, S. J., van Venrooij, W. J. & Luhrmann, R. (1996) *Nucleic Acids Res.* **24,** 4614–4623.